Estimation and Forecast of Depth-Averaged Ocean Current Using Underwater Gliders

Yaojian Zhou*†, Jiancheng Yu*, Xiaohui Wang*
*Shenyang Institute of Automation, Chinese Academy of Sciences
Shenyang,110016, P.R.China.
Email: {zhouyj,yjc,wxh}@sia.cn
†University of Chinese Academy of Sciences
Beijing, 100049, P.R.China.

***Abstract*—Depth-averaged ocean current plays a significant role in marine scientific research, in particular, which is valuable for the navigation of underwater gliders. In this paper, we study the estimation and forecast of depth-averaged ocean current using underwater gliders. By considering three factors: the seawater density difference, the pressure hull compression deformation and the unstable depth intervals of a profile, we build a model for rapid calculation of underwater gliders' horizontal speed in order to improve the accuracy of the estimated depth-averaged ocean current. Then we adopt a novel machine learning model to forecast the depth-averaged ocean current of the next profile. Compared with two rough forecasting methods commonly used in engineering, our novel forecasting model has a better performance.**

***Keywords*—Depth-averaged ocean current; Seawater density difference; Pressure hull compression deformation; LSSVM; Underwater gliders**

I. INTRODUCTION

Underwater gliders are a new class of AUVs that are driven by buoyancy, whose advantages , such as low costs, high endurance over long distances make them a good choice for a wide range of ocean observation applications. Some gliders have been commercialized such as the Slocum [1], the Seaglider [2] and the Spray[3], while other gliders have been on the stage of engineering application such as SeaWing gliders developed by Shenyang Institute of Automation (SIA), Chinese Academy of Sciences.

Depth averaged current (DAC) is the average of different-depth ocean currents in the horizontal plane. The basic way of estimating DAC is to use the difference between the dead-reckoned(DR) and measured(GPS) surfacing position which is divided by the subsurface interval[4]. In [5], the uncertainty of DR is analyzed by Unscented Kalman Filter, and then the DAC can be estimated. In lake trial, the DAC can be calculated by using a current profiler mounted on underwater gliders to improve the accuracy of DR[6]. In engineering, the most basic application of DAC is to provide assistance for glider navigation. The accuracy of positioning, tracking and planning can be greatly improved with the help of relatively precise DAC.DAC also has some other applications: compared DACs obtained by gliders with the ocean currents provided by two different ocean models, to confirm the performance of the ocean models[7]; utilize the real-time DAC to calibrate the error of the accelerometer mounted on underwater gliders[8];use DACs acquired by gliders to validate the currents observed by HF radar [9].

In the estimation of DAC, GPS positioning error is always ignored, and we think the main part of the estimating error is derived from DR. Although the horizontal speed of underwater gliders can have a great impact on DR, it is difficult to be measured because of the following reasons: to save cost, gliders are rarely willing to carry a speedometer; meanwhile, the seawater density difference and pressure hull compression deformation can lead to changes of the driven buoyancy, which can further affect the glider speed; also there exists unstable intervals of the whole profile that can not be ignored.In [10],an effective method is proposed to calculate the glider horizontal speed, but it is computationally expensive, which may cause inconvenience in practice. To estimate DAC better, we should calculate horizontal speed more quickly,while the accuracy should not be reduced.

Besides the DAC estimation, we also tend to forecast the DAC forecasting of the next dive when gliders move in the sea. This question is more difficult. On the one hand, the mechanism of DAC is complicated, which is the integration of different kinds of ocean currents within the scope of local space and time, while ocean currents are caused by many complex factors such as sea water density difference, sea wind and the tides, and on the other hand, it will cost several hours to estimate the DAC in one profile, which makes the sample size quite limited. In order to forecast DAC, some simple methods are adopted in engineering, which regard the DAC of the last profile or the average of several historical DACs as the DAC of the next profile. Obviously, those forecasting schemes are too rough, which may contain many errors.

This paper firstly introduces a estimation estimation method of DAC. In order to get more precise estimation, the seawater density difference, the pressure hull compression deformation, and the unstable intervals are all put into consideration to recalculate the horizontal speed, then the speed is used to estimate the DAC, and the effectiveness of the DAC is validated. Secondly, considering the characteristics of DAC, a novel machine learning model is adopted to forecast the DAC of the next profile.

This work is supported by National Natural Science Foundation of China, Grant No. 61233013

978-1-4673-9724-7/16/$31.00 ©2016 IEEE

II. DAC Estimating

A. Estimation Method

A underwater glider starts to dive at the position P_n, then after a diving cycle, the glider resurfaces at the position P_{n+1},which can be read by GPS. If the glider speed is known and we assume the time cost of the profile T_n, then we can get the DR resurfacing point $P_{n+1,0}$. The DAC velocity of the nth profile can be described as follow:

$$\boldsymbol{V}_{dac,n} = \frac{\overrightarrow{P_{n+1,0}P_{n+1}}}{T_n}, \tag{1}$$

where the DR resurfacing point $P_{n+1,0}$ and P_n satisfy the following equation

$$P_{n+1,0} = P_n + \sum\nolimits_{i=0}^{k} \boldsymbol{V}_i \Delta t, \tag{2}$$

where Δt is the sampling interval of the navigation system, satisfying $\sum_{i=0}^{k} \Delta t = T_n$,and $\boldsymbol{V}_i$ is the underwater glider horizontal speed at the ith sampling interval. If $\boldsymbol{V}_i$ is the same in the whole profile and we name it $\boldsymbol{V}_{avr}$, then (2) can be simplified as

$$P_{n+1,0} = P_n + \boldsymbol{V}_{avr} T_n. \tag{3}$$

B. Horizontal Speed Calculation

For saving cost, there are few underwater gliders carry speed measuring devices. When gliders move in a water column following the sawtooth motion pattern, the speed can be influenced by the following factors: the seawater density difference and pressure hull compression deformation, which can lead to changes of the driven-buoyancy and further affect changes of the glider speed; also there exists unstable intervals in the yo-yo profile that can not be ignored. As a result, it is difficult to determine the glider horizontal speed. In [10],the glider horizontal speed is calculated from the data measured by depth sensor and attitude sensor, as equation(4)

$$v_h = \frac{v_z}{\tan(\gamma)}, \tag{4}$$

where v_z is the depth rate, v_h is the horizontal speed of the glider, and γ is the gliding angle, which can be calculated by the pitching angle θ minus the attack angle α

$$\gamma = \theta - \alpha, \tag{5}$$

where α is expressed as

$$\alpha(\gamma) = \frac{K_L}{2K_D}\tan\gamma(-1+ \sqrt{1 - 4\frac{K_D}{K_L^2}\cot\gamma(K_{D0}\cot\gamma + K_{L0})}) . \tag{6}$$

The K_{L0},K_L,K_{D0},K_D in (6) are lift and drag coefficients, which can be determined by the glider's structure. The v_h in (4) is the horizontal speed in each CTD sampling interval. If there exists N sampling intervals totally, then the average of the horizontal speed of the whole profile can be described as

$$V_{avr1} = \frac{\sum_{i=1}^{N} v_h(i)}{N}. \tag{7}$$

Apparently, since a profile has too many CTD sampling intervals and each calculation of v_h need to solve a nonlinear equation, it will be cost long computing time to get V_{avr1}.

In order to satisfy the real-time requirements in sea trials, we give another rapid-calculation model for underwater glider horizontal speed, which put the factors, such as the seawater density difference, the pressure hull compression deformation, and the unstable depth intervals into consideration.

For a same glider, the unstable depth intervals are almost the same under the same configuration. If the maximum diving depth is $h_{\max}$ and the unstable depth intervals are $[0, h_1]$ and $[h_{max} - \Delta h, h_{max}]$,in which $[h_{max} - \Delta h, h_{max}]$ can be ignored because it is too small, then the stable depth interval is $[h_1, h_{max} - \Delta h]$.According to the scheme provided by [11],the additional net buoyancy caused by the seawater density difference and pressure hull compression deformation in $[h_1, h_{max} - \Delta h]$ can be expressed in the following way:

$$m_{add}(h) = \left(\sum_{i=0}^{k} p_i h^i\right)(V_{glider0} - \kappa h) - \rho_{balance} V_{glider0}, h \in [h_1, h_{\max} - \Delta h] \tag{8}$$

where $\sum_{i=0}^{k} p_i h^i$ represents the polynomial used for fitting the density of sea water, p is the fitting coefficient, k is the fitting order, h is the depth, $V_{glider0}$ is the glider neutral volume of the sea surface, κ is the coefficient which represents the pressure hull compressed with depth by linear, and $\rho_{balance}$ is the neutral density that can balance the gravity and buoyancy of the glider. Combining with m_{add} and the input net buoyancy $\pm m_b$, plugging the sum into the stable linear motion speed model[12], averaging the horizontal component of glider speed, we can obtain the average glider horizontal speed in $[h_1, h_{max} - \Delta h]$

$$V_{stable} = 0.5\sqrt{\frac{g\cos\gamma}{K_{L0} + K_L\alpha(\gamma)}}\cos\gamma \frac{\int_{h_1}^{h_{\max}-\Delta h}(\sqrt{|m_{add}(h) + m_b|} + \sqrt{|m_{add}(h) - m_b|})dh}{h_{\max} - \Delta h - h_1}. \tag{9}$$

Next we calculate the average horizontal speed $V_{unstable}$ of the unstable depth interval $[0, h_1]$.For most situations, h_1 will be less than 100m. As a result, the seawater density difference and pressure hull compression deformation can hardly have much influence on the glider speed in this interval. Hence we think the average horizontal speeds in $[0, h_1]$ of the descending part and ascending part are essentially the same. We adopt (4) to (7) to calculate the average horizontal speed in $[0, h_1]$ of the descending part, then the averaged glider horizontal speed of the whole profile V_{avr2} is

$$V_{avr2} = \frac{h_{\max} - \Delta h - h_1}{h_{\max} - \Delta h} V_{stable} + \frac{h_1}{h_{\max} - \Delta h} V_{unstable}. \tag{10}$$

III. DAC Forecating

A. Forecast principle

Generally speaking, the DACs obtained by gliders are disordered and lack of regularity.Usually, ocean currents of local areas can be forecasted by empirical forecasting models, which can be decomposed into three components: a tide component,a non-tide component and a wind-driven component(optional)[13], [14].All the components have both

temporal and spatial variations and they are quite complicated,especially the tidal component and wind-driven component. The tidal component is made up of as many as hundreds of constituents, the parameters of which need to be identified are quite a lot. Wind-driven component is related to sea wind,but the sea wind is hard to obtain,so the calculation of wind-driven current model is not easy.Ocean currents are integrated results of the above component currents, while DAC is the result of ocean currents in different time, location and depth, which is more complicated. On the other hand,it will cost several hours to get a DAC sample,and the samples of DAC are limited.Hence,it is difficult to model DAC using traditional empirical forecasting models.

Intuitively,in the scope of small area,the DAC velocity in the $n+1$ profile can be described using the historical DAC velocities, as equation(11)

$$\boldsymbol{V}_{dac}(n+1)=f\left(\boldsymbol{V}_{dac}(n),\boldsymbol{V}_{dac}(n-1),\boldsymbol{V}_{dac}(n-2),\cdots\right). \tag{11}$$

In this paper,we use the nonlinear weighted form to calculate $\boldsymbol{V}_{dac}$.In oceanographic research, the symbol u denotes flow velocity in E/W direction and v denotes flow velocity in N/S direction, We use η to denote either u or v.Then, η in the $n+1$th profile can be expressed as

$$\eta_{n+1}=\sum_{i=1}^{n} w_i\phi(\eta_i)+b, \tag{12}$$

where w_i is the weight coefficient, n is the order of model which is a positive integer,$\phi(\cdot)$ is a nonlinear mapping,and b is the offset error.

B. Forecasting model

The support vector machine (SVM) method, which was first suggested by Vapnik [15] has recently been used in a range of applications such as data mining, classification, regression and time-series forecasting. LSSVM is modified from existed SVM, which is introduced by Suykens[16]. This reformulation greatly simplifies the problem in such a way that the solution is characterized by a linear system. LSSVM is particularly suitable for time-series forecasting on the condition that the sample size is limited and the regularity is bad. In this section, we adopt the novel forecasting tool to forecast DAC.

Before using LSSVM, all the data of DAC velocities should be normalized in $[\ 0\quad 1\ ]$, which can reduce the computational complexity and avoid the large value controlling the training process. If all the data is $\boldsymbol{\eta}$, then the normalized data is

$$\bar{\boldsymbol{\eta}}=\frac{\boldsymbol{\eta}-\min(\boldsymbol{\eta})}{\max(\boldsymbol{\eta})-min(\boldsymbol{\eta})}. \tag{13}$$

On-line LSSVM is a type of LSSVM which fix the length of the data by a moving window. In [17],the training data of on-line LSSVM has the following form:$\{\mathbf{x}(K),y(K)\}$,where $\mathbf{x}(K)=[\mathbf{x}_K,\mathbf{x}_{K+1},\cdots,\mathbf{x}_{K+l-1}]$,$\mathbf{y}(K)=(y_K,y_{K+1},\cdots,y_{K+l-1})^T$,$\mathbf{x}_K\in\mathbb{R}^n$,$y_K\in\mathbb{R}$,$K$ represents the DAC of the Kth profile. As a new sample added, the oldest sample will be removed, and the sample number l keeps constant.

The on-line LSSVM model has the following expression in [17]

$$y(\mathbf{x},K)=\sum_{i=K}^{K+l-1}\boldsymbol{a}_i(K)k(\mathbf{x},\mathbf{x}_i)+\boldsymbol{b}(K), \tag{14}$$

where $\boldsymbol{a}(K)=(\boldsymbol{a}_K,\boldsymbol{a}_{K+1},\cdots,\boldsymbol{a}_{K+l-1})^T$ is the Lagrangian multiplier, $\boldsymbol{b}(K)=\boldsymbol{b}_K$ is the constant bias which needs to be solved, and $k(\mathbf{x},\mathbf{x}_i)$ is the kernel function, different kernel function corresponding to different support vector basis. Gaussian RBFs have better trade-off between accuracy and smoothness of the approximation than other radial basis functions. Therefore, we use Gaussian RBFs as the kernel functions. We use particle swarm optimization (PSO) to select the kernel parameter and regularization parameter , and the details will be showed later. The solution of the model in (14) is given below [17]

$$\begin{aligned}\boldsymbol{a}(K)&=\mathbf{U}(K)\left(\mathbf{y}(K)-\frac{\mathbf{e}1\mathbf{e}1^T\mathbf{U}(K)\mathbf{y}(K)}{\mathbf{e}1^T\mathbf{U}(K)\mathbf{e}1}\right)\\ \boldsymbol{b}(K)&=\frac{\mathbf{e}1^T\mathbf{U}(K)\mathbf{y}(K)}{\mathbf{e}1^T\mathbf{U}(K)\mathbf{e}1}\end{aligned}, \tag{15}$$

where $\mathbf{e}1=(1,1,\cdots,1)^T$,and $\mathbf{U}(K)$ can be iterated like the following way:

$$\begin{aligned}\mathbf{U}(K)&=\begin{bmatrix}0&0\\0&\mathbf{W}(K)^{-1}\end{bmatrix}+\mathbf{r}_2(K)\mathbf{r}_2(K)^T\mathbf{z}_2(K)\\ \mathbf{U}(K+1)&=\begin{bmatrix}\mathbf{W}(K)^{-1}&0\\0&0\end{bmatrix}+\mathbf{r}_3(K+1)\\ &\quad\ \mathbf{r}_3(K+1)^T\mathbf{z}_3(K+1)\end{aligned}, \tag{16}$$

where

$$\begin{aligned}\mathbf{r}_2(K)&=\left(-1,\mathbf{F}(K)^T\mathbf{W}(K)^{-1}\right)^T\\ \mathbf{z}_2(K)&=\frac{1}{f(K)-\mathbf{F}(K)^T\mathbf{W}(K)^{-1}\mathbf{F}(K)}\\ \mathbf{r}_3(K+1)&=\left(\mathbf{V}(K+1)^T\mathbf{W}(K)^{-1},-1\right)^T\\ \mathbf{z}_3(K+1)&=\frac{1}{v(K+1)-\mathbf{V}(K+1)^T\mathbf{W}(K)^{-1}\mathbf{V}(K+1)}\\ v(K+1)&=k(\mathbf{x}_{K+l-1},\mathbf{x}_{K+l-1})+1/\gamma\\ \mathbf{V}(K+1)&=[k(\mathbf{x}_{K+1},\mathbf{x}_{K+l-1}),\cdots,k(\mathbf{x}_{K+l-1},\mathbf{x}_{K+l-1})]^T\\ f(K)&=k(x_K,x_K)+1/\gamma\\ \mathbf{F}(K)&=[k(x_{K+1},x_K)+1/\gamma,\cdots,k(x_{K+l-1},x_K)]^T\\ \mathbf{W}(K)&=\begin{bmatrix}k(\mathbf{x}_{K+1},\mathbf{x}_{K+1})+1/\gamma&\cdots\\ \vdots&\ddots\\ k(\mathbf{x}_{K+1},\mathbf{x}_{K+l-1})&\cdots\\ k(\mathbf{x}_{K+l-1},\mathbf{x}_{K+1})&\\ \vdots&\\ k(\mathbf{x}_{K+l-1},\mathbf{x}_{K+l-1})+1/\gamma&\end{bmatrix}.\end{aligned}$$

The model begins to forecast DAC after $n+l$ profiles. In order to forecast the DAC as soon as possible, we hope $n+l$ as small as possible. A common method to select n or l is to test the forecast performance by different selections from small values to large values, and the Root Mean Squared Error (RMSE) is chosen as the assessment criteria. When RMSE achieves the expected value or not changes any more, the selected n or l will be the right value.

C. Selection of σ and γ

The parameters σ and γ of LSSVM have great impact on forecasting accuracy. In the parameter space,σ and γ can be valued casually, however it will result in a great difference of the forecast. In order to avoid the complexity of the exhaustive search, some scholars introduce the evolutionary algorithm into the parameter selection of LSSVM, which has a good effect[18], [19]. This paper uses PSO algorithm to optimize the two parameters σ and γ. Choosing $[\ \sigma \quad \gamma\ ]$ as the search solution, selecting the appropriate population and generation, using PSO to iterate, we can get the minimum fitness parameters for the best parameters $[\ \sigma_{best} \quad \gamma_{best}\ ]$.

PSO comes from studying the predator-prey behavior of birds, in which some particles are initialized, then iterated by a certain way until a optimization solution is obtained. At each iteration, the particle is updated by the following two extremums: individual extremum p_{best} and the global extremum g_{best}. Individual extreme is the optimal position of a particle ever been in, while global extremum is an optimal position of all particles have been in. The particle updates its velocity and position by these two extremums as the following way:

$$\begin{aligned} V_{PSO} &= w_1 \times V_{PSO} + C_1 \times Rand() \times (p_{best} - x_{PSO}) \\ &\quad + C_2 \times Rand() \times (g_{best} - x_{PSO}) \\ x_{PSO} &= x_{PSO} + V_{PSO}, \end{aligned} \tag{17}$$

where V_{PSO} is the particle current velocity and x_{PSO} is the particle current position, w_1 corresponds to the inertia weight, *Rand()* is a random number between (0,1), C_1 and C_2 are learning factors, usually $C_1 = 1.5, C_2 = 1.7$. The steps of using PSO algorithm to optimize the parameters of the LSSVM can be described as follows:

1)Initialize the PSO parameters: the population size, learning factors, the maximum number of iterations, the initial position and velocity of each particle .

2)Use on-line LSSVM with the initial particle vector $[\ \sigma \quad \gamma\ ]$ to forecast the training data,and the error can be estimated,which is used as the fitness.Compared the current fitness with the optimal fitness of the particle, if it is better, the particle's current position will be set as the best position of the particle.

3)Compare the fitness of the particle's best position with that of the group's best position. If it is better, select the particle's best position as the best position of the group.

4) Update the particle velocity and position by (17).

5) Check whether meet the end condition(the maximum number of iterations or the reset accuracy). If it is satisfied, stop the algorithm, and the found parameters are the optimal parameters; otherwise, go to step 2), and continue to a new round searching.

IV. Simulation Results

Two different gliders seawing-1000, seawing-300 and the corresponding data from the sea trial are used to demonstrate the results. We list the same coefficients of the two gliders as below:$K_{L0} = 0.1201, K_L = -448.3706, K_{D0} = -5.7192, K_D = -401.4946, V_{glider0} = 63.75L, \Delta h = 10m$, and we also list the different coefficients of the two gliders in TABLE I.

TABLE I. Different parameters of the two gliders

	$h_{\max}$ (m)	h_1(m)	$\rho_{balance}(kg/m^3)$	$\theta(^\circ)$	m_b(kg)
Seawing-1000	1000	90	1025	20	0.3
Seawing-300	300	45	1024	20	0.5

A. Speeds Comparison

30 continuous profiles of each glider are selected to calculate the horizontal speeds V_{avr1} and V_{avr2}.The results and errors are shown in Fig.1. (a), (b) corresponding to seawing-1000,while (c),(d) corresponding to seawing-300. We also list the average computation time of the two speeds in TABLE II. The simulation environment is MATLAB 2012a, and the CPU version is core_i3-2120.

TABLE II. The comparison of the CPU time to calculate V_{avr1} and V_{avr2}

	Time-CPU1(s)	Time-CPU2(s)
Seawing-1000	222.65	2.03
Seawing-300	39.81	2.62

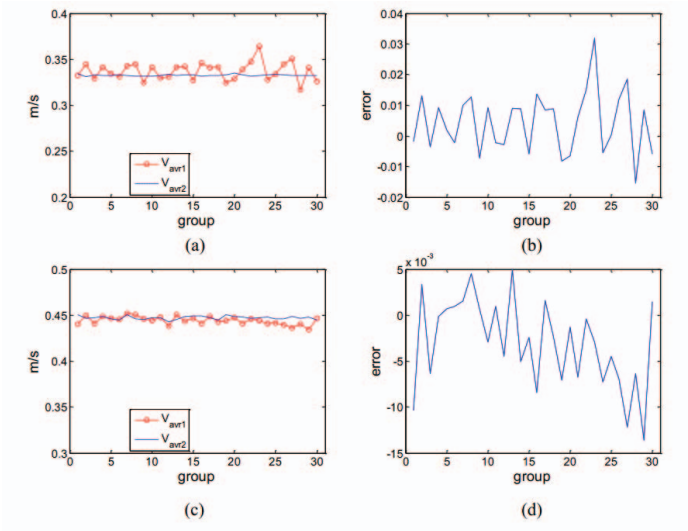

Fig. 1. The speeds and errors using two different speed calculation methods of the two gliders.

As can be seen from Fig.1. there is only little difference between V_{avr1} and V_{avr2} for each glider, but the time cost of calculating V_{avr1} is far more than that of calculating V_{avr2}.

B. DAC validity check

Using V_{avr2}, we can estimate the DACs of the two gliders, which are shown in (a) and (c) of Fig.2. To illustrate the validity of the DAC, we utilize two DR methods (One only consider the calm water, and the other regards the DAC of the last profile as the DAC of the next profile) to predict the resurfacing point. We define the distance from the two DR predictive surfacing positions to the real surfacing position (got by GPS) D1 and D2, respectively. The bar charts of D1 and D2 are shown in (b) and (d) of Fig.2.From Fig.2,we can see clearly that the DR accuracy has a great improvement with the help of DAC, which demonstrate the validity of the DAC.

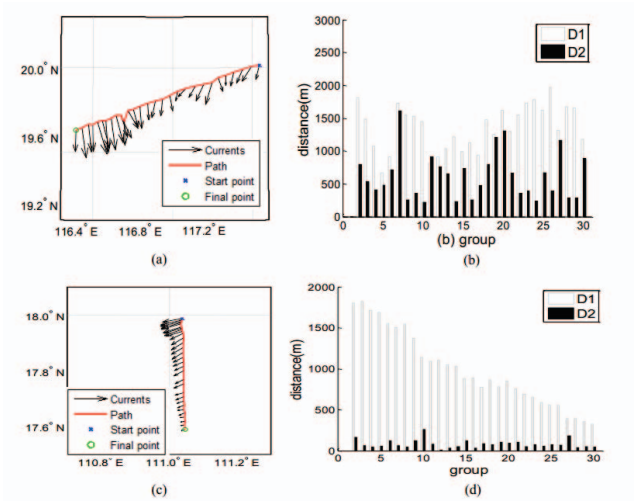

Fig. 2. Depth averaged currents and effectiveness tests of the two gliders.

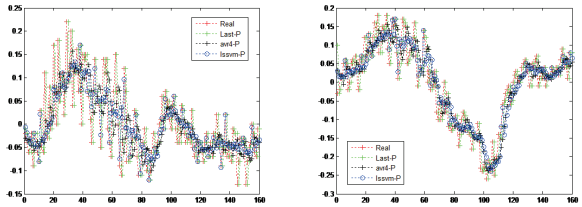

Fig. 3. The DACs forecasting of Seawing-1000, the left is u, and the right is v

C. DAC forecast

We use DAC from 160 and 100 continuous profiles of seawing-1000 and seawing-300 to test the effectiveness of the LSSVM forecasting model, and we use two coarse forecast methods commonly used in engineering for comparison, one of which use the last DAC as the DAC of the next dive, and the other use the average of the last n DACs as the DAC of the next dive. Mean Absolute Difference (MAD) and Root Mean Squared Error (RMSE) are chosen as the assessment criteria, and we set $n = 4, l = 6$. The simulation are given in TABELIII(a) to TABELIII(b) and Fig.3 to Fig.4. According to the tables and figures, it is easy to find that the performance of our novel model is better than that two course forecasting models.

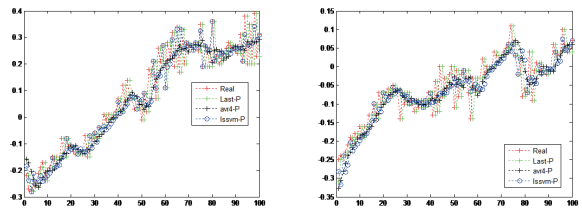

Fig. 4. The DACs forecasting of Seawing-300, the left is u, and the right is v

TABLE III. PERFORMANCE EVALUATION OF THE 3 DIFFERENT FORECASTING METHODS

(a) u of Seawing-1000

	Last-P	Avr4-P	LSSVM-P
MAD	0.0519	0.0486	0.0290
RMSE	0.0662	0.0619	0.0420

(b) v of Seawing-1000

	Last-P	Avr4-P	LSSVM-P
MAD	0.0347	0.0390	0.0287
RMSE	0.0445	0.0474	0.0380

TABLE IV. PERFORMANCE EVALUATION OF THE 3 DIFFERENT FORECASTING METHODS

(a) u of Seawing-300

	Last-P	Avr4-P	LSSVM-P
MAD	0.0611	0.0457	0.0285
RMSE	0.0826	0.0572	0.0411

(b) v of Seawing-300

	Last-P	Avr4-P	LSSVM-P
MAD	0.0338	0.0298	0.0249
RMSE	0.0460	0.0385	0.0350

V. CONCLUSION

In the deployment of underwater gliders,accurate depth averaged ocean current can bring more accurate navigation.To obtain more precise DAC,this paper studies the influence of the seawater density difference and the pressure hull compression deformation to estimate the glider horizontal speed.Combining the unstable intervals of the profile,we recalculate the horizontal speeds of two gliders,which have high accuracy and less computation time.Using the recalculated horizontal speeds,the DACs can be estimated which can further improve the navigation of the two gliders.Furthermore utilizing an effective forecasting model,on-line LSSVM can achieve the forecasting of the DACs from two gliders during the sea trials. Our novel forecasting model can be proved to provide more accurate forecast results than other two course models.

Future work will be explored to forecast DACs for the next several profiles.In addition,construct local current fields with DACs and carry out the path planning in the current fields.

REFERENCES

[1] D. C. Webb, P. J. Simonetti, and C. P. Jones, "Slocum: An underwater glider propelled by environmental energy," *IEEE Journal of Oceanic Engineering*, vol. 26, no. 4, pp. 447–452, 2001.

[2] C. C. Eriksen, T. J. Osse, R. D. Light, T. Wen, T. W. Lehman, P. L. Sabin, J. W. Ballard, and A. M. Chiodi, "Seaglider: A long-range autonomous underwater vehicle for oceanographic research," *Oceanic Engineering, IEEE Journal of*, vol. 26, no. 4, pp. 424–436, 2001.

[3] J. Sherman, R. E. Davis, W. Owens, and J. Valdes, "The autonomous underwater glider" spray"," *Oceanic Engineering, IEEE Journal of*, vol. 26, no. 4, pp. 437–446, 2001.

[4] L. Merckelbach, R. Briggs, D. Smeed, and G. Griffiths, "Current measurements from autonomous underwater gliders," in *Current Measurement Technology, 2008. CMTC 2008. IEEE/OES 9th Working Conference on*. IEEE, 2008, pp. 61–67.

[5] R. N. Smith, J. Kelly, Y. Chao, B. H. Jones, and G. S. Sukhatme, "Towards the improvement of autonomous glider navigational accuracy through the use of regional ocean models," in *ASME 2010 29th International Conference on Ocean, Offshore and Arctic Engineering*. American Society of Mechanical Engineers, 2010, pp. 597–606.

[6] P. J. Rusello, C. Yahnker, and M. Morris, "Improving depth averaged velocity measurements from seaglider with an advanced acoustic current profiler, the nortek ad2cp-glider," in *Oceans, 2012*. IEEE, 2012, pp. 1–8.

[7] C. Dobson, J. Mart, N. Strandskov, J. Kohut, O. Schofield, S. Glenn, C. Jones, D. Webb, C. Barrera, and A. Ramos, "The challenger glider mission: A global ocean predictive skill experiment," in *Oceans-San Diego, 2013*. IEEE, 2013, pp. 1–8.

[8] J. Kim, Y. Park, S. Lee, and Y. K. Lee, "Underwater glider navigation error compensation using sea current data," in *World Congress*, vol. 19, no. 1, 2014, pp. 9661–9666.

[9] A. Schaeffer and M. Roughan, "Influence of a western boundary current on shelf dynamics and upwelling from repeat glider deployments," *Geophysical Research Letters*, vol. 42, no. 1, pp. 121–128, 2015.

[10] B. Claus and R. Bachmayer, "Terrain-aided navigation for an underwater glider," *Journal of Field Robotics*, vol. 32, no. 7, pp. 935–951, 2015.

[11] Y. ZHOU, J. YU, and X. WANG, "Estimating depth average currents of underwater gliders in ocean environment," *Information and Control*, 2015,in press.

[12] X. Zhu, J. Yu, and X. Wang, "Sampling path planning of underwater glider for optimal energy consumption," *Jiqiren(Robot)*, vol. 33, no. 3, pp. 360–365, 2011.

[13] F. M. De Almeida, "The influence of wind on hf radar surface current forecasts," DTIC Document, Tech. Rep., 2008.

[14] M. H. Pickett and J. D. Paduan, "Ekman transport and pumping in the california current based on the us navy's high-resolution atmospheric model (coamps)," *Journal of Geophysical Research: Oceans*, vol. 108, no. C10, 2003.

[15] V. N. Vladimir and V. Vapnik, "The nature of statistical learning theory," 1995.

[16] J. Suykens and J. Vandewalle, "Recurrent least squares support vector machines," *Circuits and Systems I: Fundamental Theory and Applications, IEEE Transactions on*, vol. 47, no. 7, pp. 1109–1114, 2000.

[17] H.-R. Zhang and X.-D. Wang, "Incremental and online learning algorithm for regression least squares support vector machine," *CHINESE JOURNAL OF COMPUTERS-CHINESE EDITION-*, vol. 29, no. 3, p. 400, 2006.

[18] S. Chen, J. Zhu, and J. Pan, "Parameters optimization of ls-svm and its application," *JOURNAL-EAST CHINA UNIVERSITY OF SCIENCE AND TECHNOLOGY*, vol. 34, no. 2, p. 278, 2008.

[19] X. Guo, J. Yang, C. Wu, C. Wang, and Y. Liang, "A novel ls-svms hyper-parameter selection based on particle swarm optimization," *Neurocomputing*, vol. 71, no. 16, pp. 3211–3215, 2008.